Int. J. Electrochem. Sci., 17 **(2022)** Article Number: 220219, doi: 10.20964/2022.02.80

International Journal of
ELECTROCHEMICAL
SCIENCE
www.electrochemsci.org

Influence of Phosphating and Silicate Post-Sealing on Corrosion Behavior of Rebar Steel as Construction Material in Sodium Chloride Solution

Xiaojiang Yang

Capital University of Physical Education and Sports, Beijing 100091, China
E-mail: teacher_yang100@126.com

Received: 28 October 2021 / *Accepted:* 30 November 2021 / *Published:* 5 January 2022

Construction rebar steel is mainly used as the skeleton of concrete members. Improving its corrosion resistance is of great significance to ensure the stability of concrete members. In this study, zinc based phosphating and silicate sealing were combined to improve the corrosion resistance of construction rebar steel. The morphology, surface composition and corrosion resistance of rebar steel after phosphating and silicate sealing were studied. The results show that the appearance of rebar steel after phosphating and silicate sealing is black and gray. The surface components mainly include Zn, P, O, Na and Si elements. The proper concentration of sodium silicate in the sealing solution can repair the crystallization defects and improve the compactness and corrosion resistance of the phosphating film. When the concentration of sodium silicate in the sealing solution is 10 g/L, the corrosion current density of the phosphating film decreases obviously and the charge transfer resistance increases about three times. The phosphating combined with silicate sealing treatment is beneficial to prevent the penetration of corrosive medium and increase the corrosion resistance, so as to provide better corrosion protection for construction rebar steel.

Keywords: Construction rebar steel; Phosphating; Sealing; Sodium silicate; Corrosion resistance;

1. INTRODUCTION

Rebar steel is a kind of construction material which is mainly used as the skeleton of concrete members. The special structure of rebar steel can increase the friction of concrete, so improving the strength of concrete. However, the concrete members are easily eroded by chloride ions to reduce the corrosion strength of rebar steel resulting in the destruction of concrete member. In order to ensure the stability of concrete structure, it is important to improve the corrosion resistance of construction rebar steel by surface treatment. Many ways can be used to improve corrosion resistance of metal materials, such as plating, electroless deposition and so on [1-5]. However, phosphating is considered as an effective and efficient method to improve corrosion resistance of metal materials. Phosphating is a kind of pretreatment technology to form phosphate chemical conversion film by chemical and electrochemical reaction [6-10]. The phosphate conversion film is called phosphating film, which can play a better role in corrosion protection. Many researchers use phosphating technology to improve corrosion resistance of rebar steel or other construction materials reported in some literatures [11-15]. In addition to phosphating technology, sealing treatment is also a good way to increase corrosion resistance of construction materials. Common sealing technologies include chromic acid sealing, rare earth sealing, metal salt sealing and so on. Many kinds of sealing technology have been reported to improve corrosion resistance of rebar steel or construction materials [16-20]. Meanwhile, although chromic acid sealing is effective to improve corrosion resistance, the chromic acid is extremely harmful to environment. Rare earth sealing is expensive. Silicate solution is regarded as environmental protection sealing liquid which is nontoxic. Therefore, in the paper, the phosphating technology combined with silicate sealing is used to improve corrosion resistance of rebar steel as construction material which is significant and innovative. The phosphating parameters are studied and effects of silicate concentrations on surface morphology, components, corrosion resistance of rebar steel are also investigated.

2. EXPERIMENTAL

2.1 Materials and chemical agents

The sample size of construction rebar steel is 16 mm in diameter and 60 mm in length. The chemical composition is as follows: C is 0.17~0.25%, Si is 0.40~0.80%, Mn is 1.00~1.60%, P is 0.045%, S is 0.52% and the residual is Fe. The reagents used in the experiment are mainly zinc oxide, phosphoric acid, nitric acid, sodium fluoride, acetone, sodium chloride, sodium hydroxide, sodium carbonate, sodium silicate and so on. The purity grade is analytical pure.

2.2 Phosphating technology

The rebar steel sample is firstly polished by different roughness of sandpapers. After that, the rebar steel is cleaned by ultrasonic and pure water respectively. Alkaline cleaning and pickling are used to wash the surface of construction rebar steel in sequence. And then, the sample is put into the solution with 4 g/L colloidal titanium for 40 s at 30 °C. Finally, the rebar steel is immersed in phosphating solution to react for 30 min at 65 °C. The information about solution of alkaline cleaning, pickling and phosphating are listed in Tab. 1 and Tab. 2.

Table 1. Solution formula and technology parameters of alkaline cleaning and pickling

	solution formula	technology parameters
alkaline cleaning	NaOH 40 g/L Na_2CO_3 15 g/L	65 °C, 10 min
pickling	10% HCl	30 °C, 1 min

Table 2. Phosphating solution formula and technology parameters

solution formula	technology parameters
ZnO 25g/L	65 °C
H_3PO_4 40 g/L	25 min
HNO_3 24 ml/L	
NaF 1 g/L	

2.3 Silicate sealing

After phosphating, the rebar steel samples are washed and put into silicate sealing solution for 20 min at 80 °C. The concentration of sodium silicate is ranged from 4 g/L to 16 g/L to investigate the effect on performance of the rebar steel samples. The temperature of the sealing liquid is controlled constant by using the same thermostatic water bath.

2.4 Testing

A digital camera (IXUS 285HS, Canon, Japan) was used to shoot the macro morphology of the rebar steel sample, and the magnification was two times. Scanning electron microscope (MERLIN Compact, Zeiss, Germany) was used to observe the morphology of phosphating film, and energy spectrometer (X-MAX 50, Oxford, UK) was used to analyze the surface composition. Electrochemical workstation (PARSTAT, Amitate-Princeton, USA) was used to test the polarization curve and electrochemical impedance spectra of samples in 3.5% sodium chloride solution at room temperature. The rebar steel was cut to 1 cm length. And then, use the cutting machine to cut the top surface of rebar steel to a square with 1 cm ×1 cm size. Copper wires were welded to the sample and then the samples were sealed with epoxy to expose only the square surface. The three-electrode system consisted of saturated calomel electrode as the reference electrode, platinum electrode as the assistant electrode, and phosphating film sample as the working electrode. The scanning rate of polarization curve was 1 mV/s. The electrochemical impedance spectrum was scanned from 10^5 Hz to 10^{-2} Hz, and the excitation signal amplitude was 10 mV. The salt spray experiment was carried out in the salt spray chamber (Model 40A, Changzhou, China), and the experiment period was 48 hours. Ambient temperature is (35±2) °C with 5% sodium chloride solution as the corrosion medium. After the experiment, the rebar steel samples were cleaned with pure water, and the corrosion morphology was taken by digital camera.

3. RESULTS AND DISCUSSIONS

3.1 Morphology of rebar steel samples after phosphating and silicate sealing treatment

Fig.1 shows the appearance of different rebar steel samples. As can be seen from Fig.1(a), the conventional rebar steel sample is silver gray with metallic luster. It can be seen from Fig.1(b) that the phosphatized rebar steel sample is black and gray, which is different from the appearance of the conventional rebar steel sample. According to Fig.1(c)-Fig.1(e), the rebar steel sample after phosphating and sealing is also black and gray.

Figure 1. Appearance of different rebar steel samples; a-conventional rebar steel sample; b-phosphatized rebar steel sample; c-phosphatized rebar steel sample after sealing with 4 g/L sodium silicate; d-phosphatized rebar steel after sealing with 10 g/L sodium silicate; e-phosphatized rebar steel after sealing with 16 g/L sodium silicate; (auto focus with double magnification)

Fig.2 shows the surface morphology of rebar steel, phosphating film and phosphating film after sealing. It can be seen that uniform and continuous phosphating film is formed on the surface of rebar steel after phosphating treatment, but there are some defects in phosphating film, such as microcracks on the crystal surface, voids between crystals and so on resulting in poor compactness. Same surface morphology of phosphating film is reported by many researchers [21-27]. After the silicate sealing treatment, the compactness of the phosphating film is improved. For example, when the concentration of sodium silicate in the sealing solution is 10 g/L, the gap between the crystals of the phosphating film is very small after the sealing, and its compactness is the best. This is because in the sealing process, sodium silicate crystals precipitate and fill the microcracks on the crystal surface and the intercrystal gap. At the same time, the sealing liquid reacts with the phosphating film to generate silicate compounds, which can also fill the microcracks and intercrystal gap to repair the crystallization defects and improve the compactness. The mechanism of sealing is also reported in some literatures [28-32]. However, the sealing liquid is weakly alkaline. High concentration of sodium silicate enhances its alkalinity, which is difficult to repair the crystallization defect better, but will aggravate the corrosion of phoshorization film and lead to the reduction of its compactness.

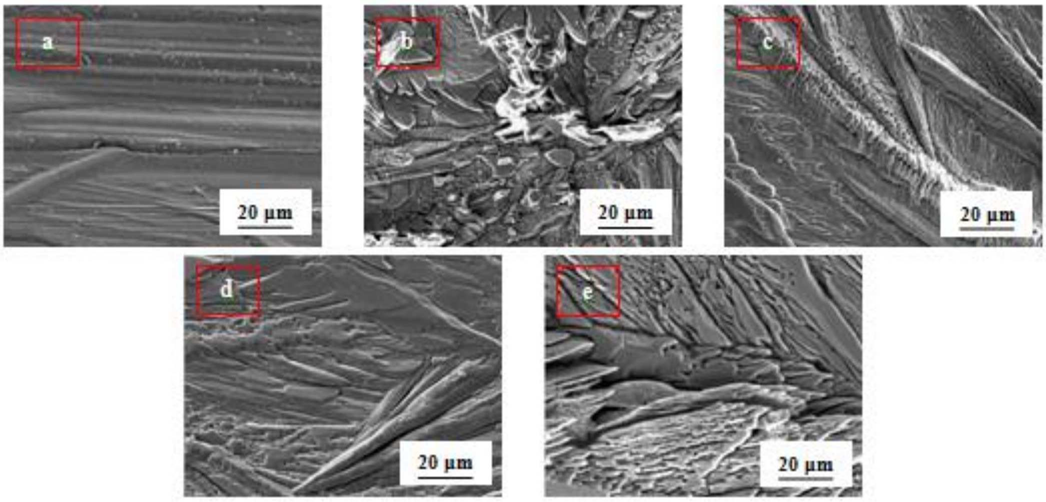

Figure 2. Surface morphology of rebar steel, phosphating film and phosphating film after sealing a-rebar steel sample; b-phosphating film; c-phosphating film after sealing with 4 g/L sodium silicate; d-phosphating film after sealing with 10 g/L sodium silicate; e-phosphating film after sealing with 16 g/L sodium silicate (sample size 6 mm×6 mm×1 mm, magnification 1500 times, accelerating voltage 10 kV)

Tab.3 shows the surface components of the phosphating film with and without silicate sealing. It can be seen that the surface components of the conventional phosphating film are mainly Zn, P and O elements, among which the mass fraction of Zn is relatively high, about 41%. After sealing, the surface components of the phosphating film are Zn, P, O, Na and Si. Meanwhile, Na and Si elements are introduced into the phosphating film through crystallization deposition and chemical reaction during the sealing process, which is consistent with the above analysis conclusions.

Table 3. Surface components of phosphating film with and without sealing

components (mass fraction, %)	phosphating film	phosphating film after silicate sealing (sodium silicate 4 g/L)	phosphating film after silicate sealing (sodium silicate 10 g/L)	phosphating film after silicate sealing (sodium silicate 16 g/L)
Zn	41.25	40.04	39.54	39.98
P	18.14	15.89	16.04	16.02
O	40.61	41.25	40.05	40.53
Na	-	2.35	3.16	2.79
Si	-	0.47	1.21	0.68

Fig.3(a) shows the EDS spectrum of the conventional phosphating film. The characteristic diffraction peaks of Zn, P and O elements can be seen, which indicate that these three elements are the main components of the conventional phosphating film. Fig.3(b) shows the EDS spectrum of the phosphating film after silicate sealing with 10 g/L sodium silicate in the sealing solution. The characteristic diffraction peaks of Zn, P, O, Na and Si can be seen, but the characteristic diffraction peak intensity of Si element is significantly lower than that of Zn, P and O elements.

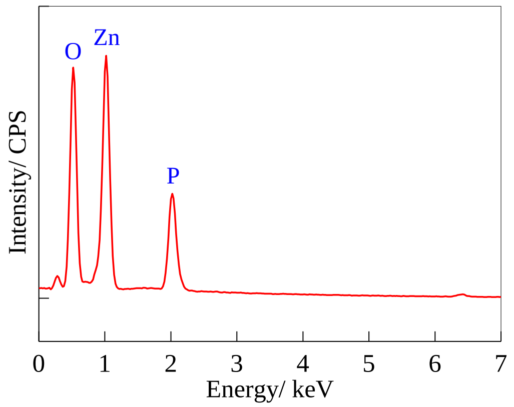

(a) phosphating film

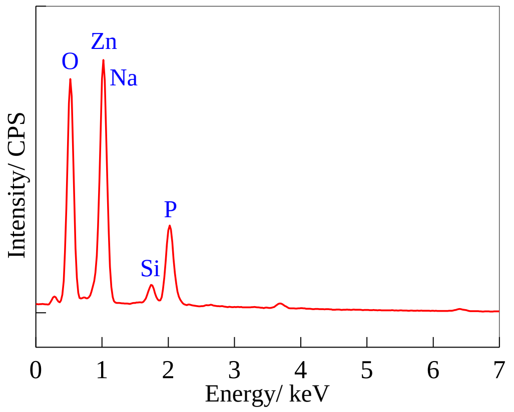

(b) phosphating film after sealing with 10 g/L sodium silicate

Figure 3. EDS spectrum of the phosphating film with and without silicate sealing; (surface scanning mode, acceleration voltage 5 kV, sampling depth 1 μm)

3.2 Corrosion resistance

3.2.1 Polarization curves analysis

Fig.4 shows the polarization curves of rebar steel, phosphating film and phosphating film after sealing treatment. Tab.4 shows the fitting results of polarization curves. The corrosion potential of rebar steel is -607.8 mV and the corrosion current density is 4.12×10^{-5} A/cm^2. Compared with rebar steel, the corrosion potential of conventional phosphating film moves to positive position, and the corrosion current density decreases obviously. After sealing treatment, the corrosion potential of the phosphating film moves further to positive position, and the corrosion current density decreases sharply. With the increase of the concentration of sodium silicate in the sealing solution, the corrosion current density shows a trend of first decreasing and then increasing. When the concentration of sodium silicate in the sealing solution is 10 g/L, the phosphating film after sealing has the most positive corrosion potential and the lowest corrosion current density equal to -504.6 mV and 1.3×10^{-6} A/cm^2 respectively.

Phosphating treatment can reduce the corrosion tendency of rebar steel and effectively improve its corrosion resistance. As phosphating film is a nonconductive insulating layer, it can inhibit the formation of microcells on the surface of rebar steel and prevent the penetration of corrosive media from the surface to the interior resulting in improvement of the corrosion resistance. After silicate sealing treatment, the corrosion tendency of rebar steel is further weakened and its corrosion resistance is better. The sealing treatment could repair the crystallization defects of phosphating film to greatly hinder the infiltration process of the corrosive medium leading to increase of corrosion resistance. Moreover, sealing treatment improves the compactness of phosphating film and reduces the contact area with corrosive medium to further improve corrosion resistance. The effect of phosphating and sealing on the corrosion resistance of materials has been reported by many people. [33-36]

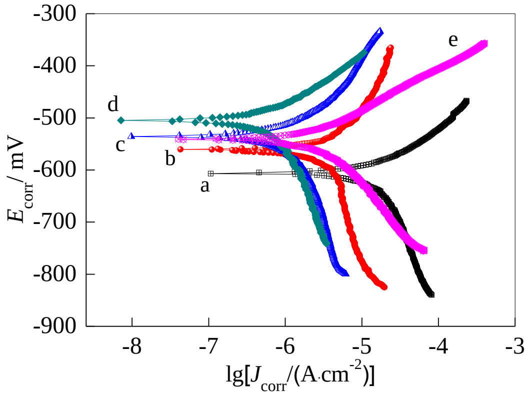

Figure 4. Polarization curves of rebar steel, phosphating film and phosphating film after sealing in sodium chloride solution; a-rebar steel; b-phosphating film; c-phosphating film after sealing with 4 g/L sodium silicate; d-phosphating film after sealing with 10 g/L sodium silicate; e-phosphating film after sealing with 16 g/L sodium silicate (saturated calomel electrode as the reference electrode, platinum electrode as the assistant electrode, and phosphating film sample as the working electrode, electrolyte is 3.5% sodium chloride solution, scanning rate of polarization curve is 1 mV/s)

Table 4. Corrosion potential and corrosion current density of rebar steel, phosphating film and phosphating film after sealing treatment

samples	E_{corr}/ mV	J_{corr}/ (A·cm^{-2})
rebar steel	-607.8	4.1×10^{-5}
phosphating film	-560.3	7.9×10^{-6}
phosphating film after silicate sealing (sodium silicate 4 g/L)	-535.9	3.3×10^{-6}
phosphating film after silicate sealing (sodium silicate 10 g/L)	-504.6	1.3×10^{-6}
phosphating film after silicate sealing (sodium silicate 16 g/L)	-541.0	3.6×10^{-6}

3.2.2 Electrochemical impedance spectroscopy analysis

Fig.5 shows the electrochemical impedance spectra of rebar steel, phosphating film and phosphating film after sealing treatment. It can be seen from Fig.5(a) that the Nyquist plots of rebar steel, phosphating film and phosphating film after sealing all present approximately semicircular capacitive reactance arc. phosphating treatment increases the capacitive reactance arc radius of rebar steel and increases the charge transfer resistance from 824.5 $\Omega\cdot cm^2$ to 2319.4 $\Omega\cdot cm^2$, as shown in Table 5. After sealing treatment, the arc radius of capacitive reactance increases further. With the increase of sodium silicate concentration in sealing solution, the arc radius of capacitive reactance and the charge transfer resistance both increase first and then decrease. When the concentration of sodium silicate in sealing solution is 10 g/L, the sealed phosphating film has maximum arc radius and charge transfer resistance of 3728.6 $\Omega\cdot cm^2$, which is at least 3 times higher than that of rebar steel. This is because the proper concentration of sodium silicate in the sealing liquid can better repair the crystallization defect and improve the compactness of the phosphating film to effectively prevent the penetration of corrosive media and increase the corrosion resistance, thus improving the impedance and corrosion resistance.

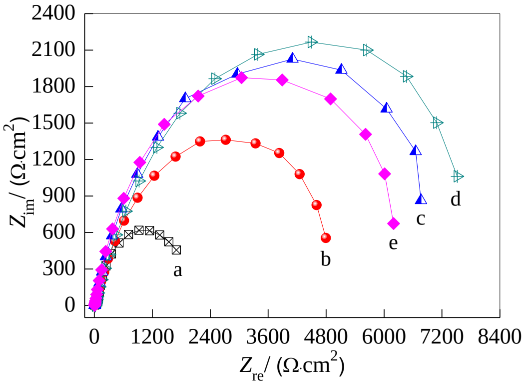

(a) Nyquist image

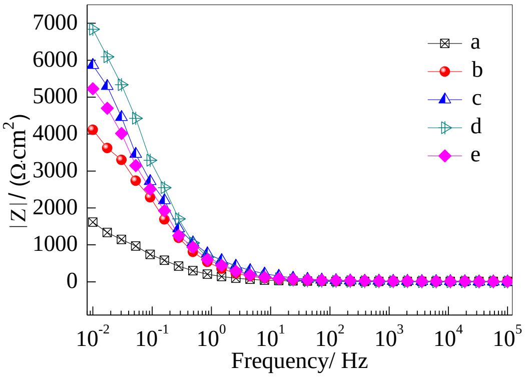

(b) Bode image

Figure 5. Electrochemical impedance spectroscopy of rebar steel, phosphating film and phosphating film after sealing; a-rebar steel; b-phosphating film; c-phosphating film after sealing with 4 g/L sodium silicate; d-phosphating film after sealing with 10 g/L sodium silicate; e-phosphating film after sealing with 16 g/L sodium silicate (scanning from 10^5 Hz to 10^{-2} Hz, the excitation signal amplitude is 10 mV, electrolyte is 3.5% sodium chloride solution)

It can be seen from Fig.5(b) that the impedance values of rebar steel, phosphating film and phosphating film after sealing all decrease with the increase of frequency, but phosphating treatment can improve the low frequency impedance values of rebar steel. After sealing treatment, the low frequency impedance value is higher. Especially, when the concentration of sodium silicate in sealing solution is 10 g/L, the low frequency impedance value reaches 6839 $\Omega\cdot cm^2$, which further confirms that the surface of rebar steel after phosphating and sealing treatment shows better corrosion resistance.

Table 5. Charge transfer resistance of rebar steel, phosphating film and phosphating film after sealing treatment

samples	charge transfer resistance/ ($\Omega\cdot cm^2$)
rebar steel	824.5
phosphating film	2319.4
phosphating film after silicate sealing (sodium silicate 4 g/L)	3221.7
phosphating film after silicate sealing (sodium silicate 10 g/L)	3728.6
phosphating film after silicate sealing (sodium silicate 16 g/L)	3029.0

3.2.3 Salt spray analysis

Fig.6 shows the appearance of different rebar steel samples after 48 h salt spray testing. As can be seen from Fig. 6(a), the surface of the conventional rebar steel sample is badly corroded which is full of russet rust spots. Fig.6(b) shows that the surface of the rebar steel sample is also corroded after phosphating, but the area covered by brown rust spot is small, which indicates that phosphating treatment can effectively improve the corrosion resistance of rebar steel. According to the Fig.6(c) to Fig.6(e), the corrosion degree of the rebar steel sample after sealing is reduced, and few brown rust spots are formed. When the concentration of sodium silicate in the sealing solution is 10 g/L, the rebar steel sample is still black and gray on the whole and only fewer rust in a small local area. It is further confirmed that the corrosion resistance of phosphorzation and sealing rebar steel sample is better when the concentration of sodium silicate in sealing solution is appropriate.

Figure 6. Appearance of different rebar steel samples after 48h salt spray testing in 5% sodium chloride solution; a-conventional rebar steel sample; b-phosphatized rebar steel sample; c-phosphatized rebar steel sample after sealing with 4 g/L sodium silicate; d-phosphatized rebar steel after sealing with 10 g/L sodium silicate; e-phosphatized rebar steel after sealing with 16 g/L sodium silicate (auto focus with double magnification)

4. CONCLUSIONS

Phosphating treatment generates a layer of non conductive film on the surface of rebar steel. The surface composition mainly includes Zn, P and O elements, which can prevent the penetration of corrosive media to improve the corrosion resistance of rebar steel. After phosphating and silicate sealing treatment, corrosion resistance of rebar steel is better. The reason is attributed to the reaction products in the sealing process to repair the crystallization defect of the phosphating film resulting in the improvement of the compactness and density. When the concentration of sodium silicate in sealing solution is 10 g/L, the phosphating film after sealing has the most positive corrosion potential and the lowest corrosion current density equal to -504.6 mV and 1.3×10^{-6} A/cm^2 respectively.

References

1. Y. D. Yu, X. X. Zhao, M. G. Li, G. Y. Wei, L. X. Sun and Y. Fu, *Surf. Eng.*, 29 (2013) 743.
2. Y. H. Hu, Y. D. Yu, H. L. Ge, G. Y. Wei and L. Jiang, *Int. J. Electrochem. Sci.*, 14 (2019) 1649.
3. J. H. Park, D. Kosugi, T. Hagio, Y. Kamimoto and R. Lchino, *Surf. Coat. Tech.*, 389 (2020) 125567.
4. L. Y. Li, J. Wang, J. Xiao, J. Yan, H. Y. Fan, L. Sun, L. Xue and Z. H. Tang, *Int. J. Hydrogen. Energ.*, 46(2021) 11849.

5. Y. D. Yu, G. Y. Wei, L. Jiang and H. L. Ge, *Int. J. Electrochem*. Sci., 15 (2020) 1108.
6. Q. Y. Qian, F. Wang, X. K. Zhang and Q. P. Zhao, *Inorg. Chem. Commun*., 127 (2021) 108555.
7. R. X. Han, L. X. Guan, S. Zhang, Y. F. Lin and J. G. Tao, *Electrochim. Acta*, 368 (2021) 137690.
8. Y. F. Zhang and S. J. Park, *J. Catal*., 394 (2021) 332.
9. D. Zhou, J. G. Yi, X. D. Zhao, J. Q. Yang, H. R. Lu and L. Z. Fan, *Chem. Eng. J*., 413 (2021) 127508.
10. X. Wang, C. Jiang, W. Z. Zhang, X. S. Wang, X. Y. Liu, B. Q. Dong and Y. X. Zhang, *Appl. Surf. Sci*., 532 (2020) 147437.
11. X. J. Jia, J. F. Song, B. Q. Xiao, Q. Liu, H. Zhao, Z. Y. Yan, J. Liao, L. Y. Wu, B. Jiang, A. Atrens and F. S. Pan, *J. Mater. Res. Technol*., 14 (2021) 1739.
12. H. Tang, J. S. Qian, Z. W. Ji, X. B. Dai and Z. Li, *Constr. Build Mater*., 255 (2020) 119422.
13. Q. Wu, B. X. Yu, P. Zhou, T. Zhang and F. H. Wang, *Mater. Chem. Phys*., 273 (2021) 125121.
14. N. Wint, C. M. Griffiths, C. J. Richards, G. Williams and H. N. Mcmurray, *Corros. Sci*., 174 (2020) 108839.
15. H. L. Liu, Z. P. Tong, Y. Yang, W. F. Zhou, J. N. Chen, X. Y. Pan and X. D. Ren, *J. Alloy. Compd*., 865 (2021) 158701.
16. L. Yang, X. H. Shi, X. F. Tian, X. Han, J. R. Mu and L. H. Qi, *Surf. Coat. Tech., 423 (2021) 127627.*
17. S. Hong, Z. Y. Wei, K. L. Wang, W. W. Gao, Y. P. Wu and J. R. Lin, *Ultrason. Sonochem*., 72 (2021) 105438.
18. R. X. Wang, L. S. Wang, C. Y. He, M. Lu and L. Sun, *Surf. Coat. Tech*., 360 (2019) 369.
19. Y. Zhang, Z. H. Wang, Y. Shi, Y. F. Shao and C. Y. Gu, *Ceram. Int*., 45 (2019) 24545.
20. Z. H. Chen, T. Dong, W. W. Qu, Y. Ru, H. Zhang, Y. L. Pei, S. K. Gong and S. S. Li, *Corros. Sci*., 156 (2019) 161.
21. M. Manna, I. Chakrabarti, N. Bandyopadhyay, *Surf. Coat. Tech*., 201 (2006) 1583.
22. M. Manna, *Corros. Sci*., 51 (2009) 451.
23. R. X. Li, Q. M. Yu, C. P. Yang, H. Chen, G. X. Xie and J. Y. Guo, *J. Clean. Prod*., 18 (2010) 1040.
24. J. Liu, B. Zhang, W. H. Qi, Y. G. Deng and R. D. K. Misra, *J. Mater. Res. Technol*., 9 (2020) 5912.
25. H. Feng, X. Y. Zhao, L. Li, X. C. Zhao and D. Y. Gao, *Constr. Build. Mater*., 291 (2021) 123316.
26. M. Z. Wang, R. Ma, A. Du, S. H. Hu, M. Muhammad, X. M. Cao, Y. Z. Fan, X. Zhao and J. J. Wu, *Mater. Chem. Phys*., 250 (2020) 123056.
27. M. Padma, S. Shanmugam and K. Ravichandran, *Surf. Interfaces*, 20 (2020) 100547.
28. Y. Y. Xu and B. L. Lin, *T. Nonferr. Metal. Soc*., 17 (2007) 1248.
29. L. L. Bi, T. L. Jin and G. Kong., *Surf. Coat. Tech*., 202 (2008) 1831.
30. Y. D. Yu, H. L. Ge, G. Y. Wei, L. Jiang and D. Zhang, *Surf. Rev. Lett*., 27 (2020) 2050020-1.
31. M. M. Liu, H. X. Hu and Y. G. Zheng, *Surf. Coat. Tech*., 309 (2017) 579.
32. B. L. Lin and J. T. Lu, *T. Nonferr. Metal. Soc*., 24 (2014) 2723.
33. D. M. Bastidas, M. Criado, S. Fajardo, A. L. Lalesia and J. M. Bastidas, *Cem. Concr. Compos*., 61 (2015) 1.
34. M. Tamilselvi, P. Kamaraj, M. Arthanareeswari and S. Devikala, *Appl. Surf. Sci*., 327 (2015) 218.
35. B. Ramezanzadeh, H. Vakili and R. Amini, *Appl. Surf. Sci*., 327 (2015) 174.
36. M. Kazami, I. Danaee and D. Zaarei, *Mater. Chem. Phys*., 148 (2014) 223.